GEOPHYSICAL RESEARCH LETTERS, VOL. 24, NO. 24, PAGES 3281-3284, DECEMBER 15, 1997

Chronology of the episode 54 eruption at Kilauea Volcano, Hawaii, from GOES-9 satellite data

Andrew J. L. Harris, Laszlo Keszthelyi,[1] Luke P. Flynn, and Peter J. Mouginis-Mark

Hawaii Institute of Geophysics and Planetology, University of Hawaii, Honolulu

Carl Thornber, James Kauahikaua, David Sherrod, and Frank Trusdell

U.S. Geological Survey, Hawaiian Volcano Observatory, Hawaii National Park

Michael W. Sawyer and Pierre Flament

Department of Oceanography, University of Hawaii, Honolulu

Abstract. The free availability of GOES satellite data every 15 minutes makes these data an attractive tool for studying short-term changes on cloud-free volcanoes in the Pacific basin. We use cloud-free GOES-9 data to investigate the chronology of the January 1997, episode 54 eruption of Kilauea Volcano, Hawaii. Seventy-six images for this effusive eruption were collected over a 60-hour period and show the opening and shutdown of active fissures, the draining and refilling of the Pu'u 'O'o lava lake, and the cessation of activity at the ocean entry.

Introduction

Many active volcanoes around the globe are poorly monitored, and eruptions often occur in remote or inaccessible regions. Detecting the onset and cessation of volcanic activity is often difficult. Thermal data from Geostationary Operational Environmental Satellites (GOES) provide a readily available method to address this detection problem. While GOES data have already been used to monitor explosive eruptions [e.g., *Glaze et al*, 1989; *Holasek and Self*, 1995; *Rose et al.*, 1996], we now show that such data are also useful for studying effusive activity. GOES-8 and -9 data are available for North America every 15 minutes, in near-real time, at a spatial resolution of ~4-km/pixel. While the instrument detectors are unable to observe hot spots through clouds, they do provide essentially hemispheric coverage by day and night. As such, these satellite observations could be valuable in deciding when and where to dispatch field teams during future eruptions of remote, unmonitored, or large volcanoes such as Mauna Loa (Hawaii). Here we demonstrate the ability to study effusive eruptions using 76 images acquired during the January 30-31, 1997 episode 54 eruption of Kilauea Volcano, Hawaii.

GOES Data for Monitoring Effusive Eruptions: A Case Study

Episode 54 of the ongoing 14-year eruption of Kilauea Volcano consisted of 22 hours of intermittent fissure activity [*Thornber et al*, 1997]. Six separate fissures totaling ~2.3 km in length fed short (<0.8 km long) flows that covered an area of 0.239 km^2 (Figure 1a; Table 1). Prior to this episode, the eruption was in a steady state, feeding lava from the Pu'u 'O'o cone to the ocean through 10 km of stable lava tubes, with occasional surface flows.

The GOES-9 Imager has 5 channels covering 0.52-12.5 µm. For active lava detection the most useful channels are 2 (3.78-4.03 µm) and 4 (10.2-11.2 µm). In particular, channels in the 3.5-4.0 µm waveband are very sensitive to subpixel volcanic hot spots [e.g., *Wiesnet and D'Aguanno*, 1982; *Mouginis-Mark et al.*, 1994; *Harris et al.*, 1995a]. We use the visible channel (channel 1: 0.55-0.75 µm) to carry out a preliminary visual cloud check, allowing us to reject cloud-contaminated images. To locate thermal anomalies due to active lava on cloud-free images, we subtract brightness temperatures derived from channel 4 from those derived from channel 2, a procedure that highlights subpixel hot spots and removes the effects of solar heating [*Harris et al.*, 1995b; Figure 2].

Prior to episode 54, activity at Kilauea was evident in the GOES data as a thermal anomaly located at the coast (Figure 1b; 2a). This pre-episode 54 anomaly was due to lava entering the ocean, tube-fed lava visible through skylights, and lava at surface breakouts along the tube system. The GOES-9 image acquired at 0243 (all times are Hawaiian Standard Time) on 30 January 1997 showed a second anomaly, directly NW of the ocean entry anomaly, in the vicinity of Napau Crater (Figures 1c and 2b). This marks the start of the episode 54 effusive activity as lava erupted from fissures A, B, and C (Figure 1a). On subsequent images this

Table 1. Episode 54 eruptive chronology from ground and GOES observations. All times are in Hawaiian Standard Time and give the times that activity began and ended as observed from the ground and GOES data. For the GOES timings, a range is given for each start and stop time. These ranges are set using images between which marked rises or declines in R_{2volc} were observed. Date (in parentheses) give month/day of activity.

Fissure	Ground Time Active	GOES Start Time	GOES Stop Time
A	0240-0530 (1/30)	0228-0243	0713-0728
B	>0240 -0716 (1/30)	0258-0313	0713-0728
C	>0240-0630 (1/30)	0258-0313	0713-0728
D	1239-1450 (1/30)	1158-1228	1513-1528
E	1639-1840 (1/30)	1628-1643	1858-1913
F	2043-0033 (1/31)	2028-2043	2328-0033
Pu'u 'O'o	0740 (2/24)	0643-0658	to current (10/97)

[1]Also at U.S. Geological Survey, Hawaiian Volcano Observatory, Hawaii National Park.

Paper number 97GL03165.
0094-8534/97/97GL-03165$05.00

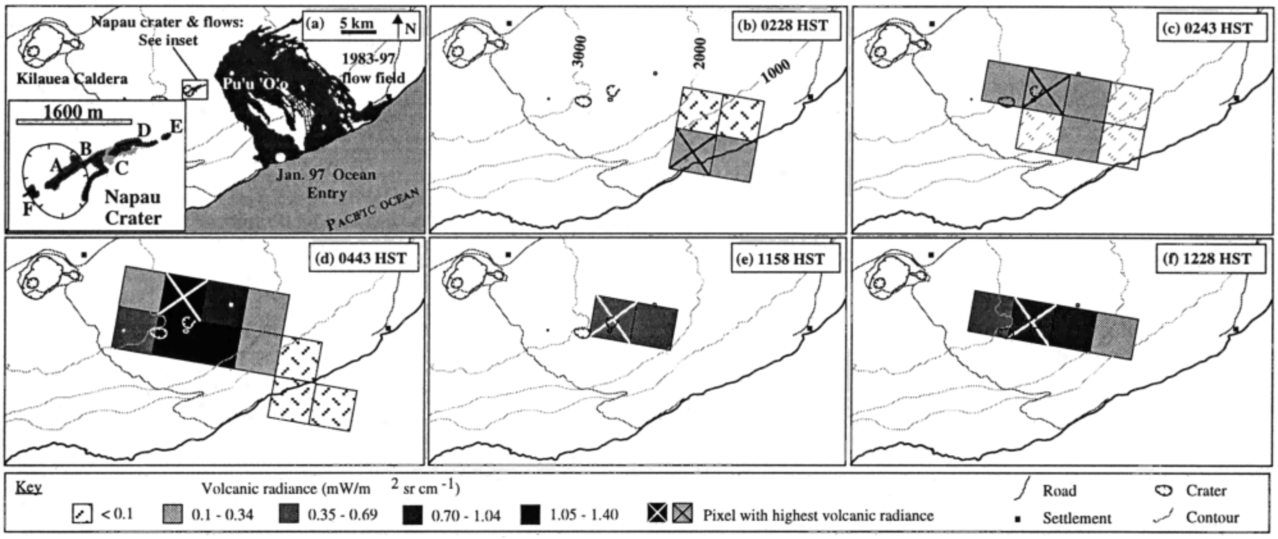

Figure 1. GOES hot spot pixels fitted to a map of Kilauea's east rift zone. (a) gives the location of the 1983-1997 flow field, the ocean entry in January 1997, and the episode 54 eruptive fissures (enlarged as inset). (b) locates the pre-episode 54 anomaly that resulted from active lava at the ocean entry. (c) and (d) locate the increasingly radiant pixels at Napau Crater caused by the episode 54 activity, as well as the less intense hot spot at the coastal ocean entry. By (e) the shutdown of the eruption is apparent from a decrease in the size and intensity of the Napau Crater anomaly. Activity at fissure D is marked by an increase in size and intensity of the anomaly (f).

anomaly increased in size and intensity with a smaller, less intense anomaly associated with the ocean entry still located at the coast (Figure 1d; 2b-f). From 0713 the Napau anomaly began to decrease in size and intensity, a trend which continued throughout the morning of 30 January (Figure 1e; 2g-i). This decline corresponds with our field observations of decreased activity between 0530 and 0716. After 1158 the size and intensity of the Napau anomaly in the GOES data increased again (Figure 1f; 2j-k). This revival was nearly coincident with our field observations of the opening of a fourth eruptive fissure (fissure D, Figure 1a).

A quantitative analysis of the GOES images allows the timing of most of the volcanic events during episode 54 (Figure 3; Table 1). In order to isolate the signal caused by volcanic activity we subtracted the lowest channel 2 radiance for any pixel immediately surrounding the anomaly from the highest channel 2 radiance occurring within the anomaly. This method produces a normalized measure of volcanic spectral radiance (R_{2volc}), independent of seasonal or diurnal ambient temperature variations. Because the channel 2 pixel radiance is the integrated radiance (R_2), composed of contributions from several subpixel sources, variations in the background temperature and the temperature and/or size of any lava bodies may change R_2. By calculating R_{2volc} we remove the influence of the nonactive background, producing a value that is comparable between images so that it can be used to study temporal change.

Prior to 30 January 1997, lava from a vent on the west flank of Pu'u 'O'o fed a well-established tube system which extended to the coast. In the week prior to episode 54, R_{2volc} at the ocean entry was 0.26 ± 0.17 mW/m^2-sr-cm^{-1} (in which sr = steradian). However, around 2100 on 28 January, R_{2volc} doubled to 0.52 ± 0.17 mW/m^2-sr-cm^{-1} (Figure 3a). This higher level persisted until midday on 29 January and coincided with two surface breakouts inland of the ocean entry. We are unable to determine the exact timing of this event because GOES images prior to 2100 on 28 January were cloudy. The first ground reports of these breakouts were not until 1045 on 29 January. An increase in R_{2volc} to the highest levels in the time series (1.46 mW/m^2-sr-cm^{-1}, Figures 3a and b) was obvious from cloud-free images covering the start of episode 54.

The episode 54 eruption was witnessed by two hikers who estimated its onset at around 0240. The appearance of the anomaly in the vicinity Napau Crater in GOES data between 0228 and 0243 (Figures 1 and 2) confirms this observation. No ground party saw the beginning of the eruption, so there is uncertainty over the timing of the opening of fissures A-C (Table 1). We suggest that initial low R_{2volc} between 0228 and 0258 represents activity from fissure A. The marked R_{2volc} increase after 0258 (Figure 3b) could result from a sudden increase in lava area as fissures B and C opened and began fountaining. In the absence of field observations, however, we are unable to confirm this speculated sequence of events.

Fissures A and C had shut down at 0530 and 0630 respectively, but we are unable to identify these events in the GOES data because the continued activity at fissure B was sufficient to saturate channel 2 (Figure 3b). During episodes of intense effusive activity GOES channel 2 becomes saturated, setting an upper limit to R_{2volc}. However, we note an end to saturation and decline in R_{2volc} between 0713 and 0728 (Figure 3b), coincident with the observed shut down of fissure B at 0716 (Table 1).

Activity resumed in the early afternoon at fissure D. This was marked by a renewal of saturation in channel 2. The first image to show saturation associated with the fissure D event was acquired at 1228 (Figure 3b), indicating that fissure D opened between 1158 and 1228. This is earlier than the field reports, which describe this fissure becoming active at 1239. By this time, however, lava fountaining was already underway, and it is likely that the opening of fissure D did take place prior to 1228. Unfortunately there was no 1213 image to better constrain this time because the sensor was in full disc mode. During full disc mode, which is switched to once every 3 hours, an image of the whole Earth disc is acquired. The process takes 18 minutes to complete. At all other times, smaller images covering the latitudes

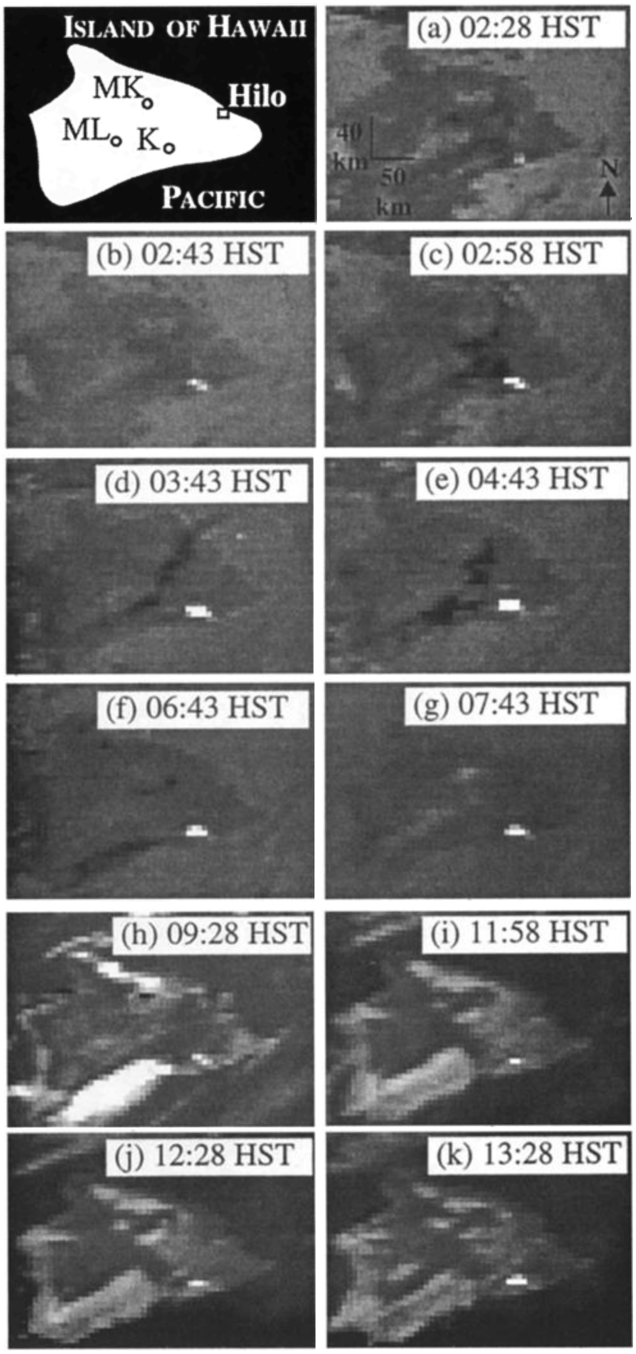

Figure 2. GOES channel 2 minus channel 4 brightness temperature images acquired during 30 January 1997 show the evolution of the hot spot resulting from effusive activity at the episode 54 fissures in Napau Crater. In each case the hot spot is apparent as a group of bright pixels on the south coast of the Island of Hawaii. Large bright areas SW of the hot spot after (h) are cloud. (a) was acquired prior to episode 54 and show a less intense coastal hot spot due to active lava at the ocean entries. This hot spot can be identified as a less intense anomaly immediately SE of the Napau Crater anomaly on (b) to (g). N.B. (1) Although 4 km/pixel is the nominal resolution, the viewing geometry for Hawaii (5.5° off nadir) means that pixels are ~5.5 km across at this location. (2) Although each GOES-9 scan begins at approximately 10, 25, 40 and 55 minutes past the hour, pixels at Hawaii's latitude are not acquired until 13±1, 28±1, 43±1 and 58±1 minutes after the hour.

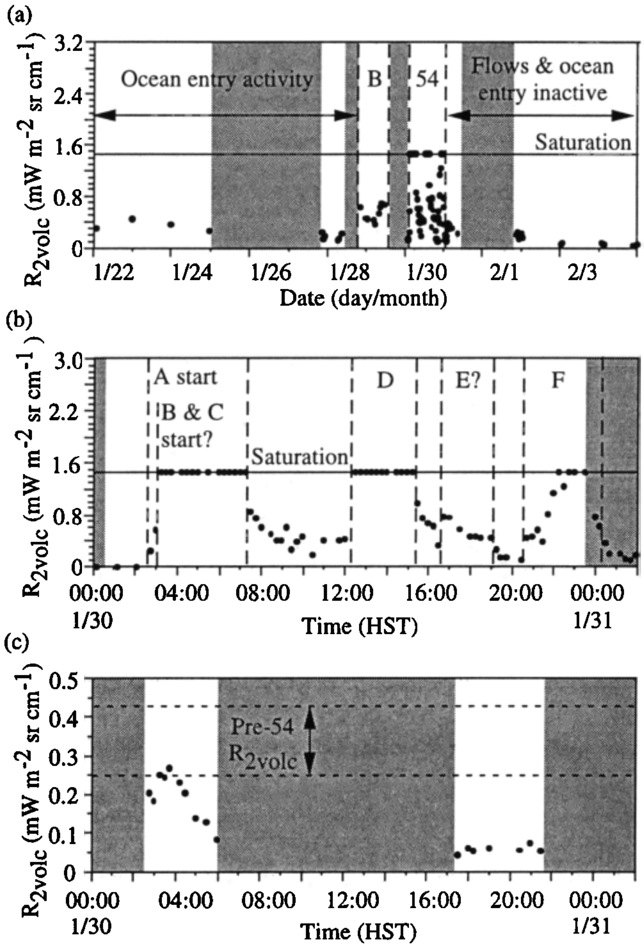

Figure 3. (a) Time series of R_{2volc} produced over a two-week period straddling the episode 54 eruption. Elevated R_{2volc} due to breakouts from the tube system and the fissure-fed flow activity at Napau Crater during episode 54 are marked "B" and "54" respectively. The slightly elevated value on January 23 is coincident with lava breakouts observed ~7 km inland from the ocean entry at 1300 on this day. (b) and (c) respectively give R_{2volc} time series produced for the hottest pixel within the Napau Crater anomaly and the ocean entry anomaly during the episode 54 eruption. Periods of effusive activity apparent from changes in the level of R_{2volc} are marked with vertical dashed lines, and the eruptive fissure to which each relates are indicated. On (c) the pre-episode 54 range of R_{2volc} obtained for ocean entry pixels is given. Note that an upper limit to R_{2volc} of 1.46 mW/m^2-sr-cm^{-1} is set by saturation. On all three figures gray boxes indicate cloud cover.

of the United States are acquired every 15 minutes. The end of the fissure D activity is indicated by a decrease in R_{2volc} between 1513 and 1528. This is 15-30 minutes later than the ground report. This minor discrepancy is readily explained by the heat from the now inactive, but relatively large and still hot, channelized flow that drained into an inactive fissure after the cessation of fissure D.

Between 1639 and 1840, lava issued from fissure E (Figure 1a). Fissure E flows only covered 0.004 km^2 as compared to 0.03 - 0.16 km^2 for the other flows. As a result, the observed activity produced only a minor increase in R_{2volc} between 1628 and 1643 (Figure 3b). A drop in R_{2volc} between 1858 and 1913 corresponds to the end of spattering along fissure E.

The final phase of episode 54 activity was at fissure F (Figure 1a), and produced an increase in R_{2volc} between 2028 and 2043, followed by a rise to saturation by 2200 (Figure 3b). This corresponds well with the observed start time of 2043 in the field. The sharp drop in R_{2volc} between 2328 and 2358 (Figure 3b) is not caused by the termination of activity at this time. Instead, this drop is caused by thin or broken clouds entering the scene which absorb or scatter upwelling radiation. Ground observations show that this fissure persisted until 0033 on 31 January, when a second drop in R_{2volc} occurs (Figure 3b). To avoid inaccurate conclusions, such cloud-induced declines in radiance must be identified. We achieve this by checking the visible channel (channel 1) for cloud during periods of declining radiance. Following this event, no further increases in R_{2volc} were observed; R_{2volc} declined rapidly to the lowest levels in the series (0.13±0.1 mW/m^2-sr-cm^{-1}, Figure 3a). These low-level thermal emissions are related to the inactive, cooling flows around Napau Crater.

Prior to episode 54, reflected glow at night from a lava pond within the Pu'u 'O'o cone was clearly visible. However, observations from the main road between Hilo and Volcano (Highway 11) at 2200 on 29 January revealed no glow, indicating drainage of the pond. From the Hawaiian Volcano Observatory (HVO) seismic record we speculate that draining began at 1841, an event which would have robbed the flank vent of its lava source. This would also have preceded the collapse of the Pu'u 'O'o cone, which most probably occurred at 1915 when a sudden tremor burst occurred and a "loud whooshing roar" was reported from Glenwood (on Highway 11). The collapse no doubt resulted from the tremor associated with drainage of the pond and the sudden lack of crater wall support.

The R_{2volc} calculated for the ocean entry anomaly during the eruption shows a decline after 0343 (Figure 3c), indicating drainage of the tube-system after the Pu'u 'O'o feeding vent had shut down. This is consistent with field observations showing that the entries can take 6 hours to respond to pauses in supply from the Pu'u 'O'o vent and that it can take up to 24 hours for flow to cease at the entries following supply shut-down.

Following episode 54, no active lava was observed at the surface until 0740 on 24 February, when helicopter pilots reported that a small active lava pond had been re-established within Pu'u 'O'o. This event was also recorded in the GOES data. No GOES thermal anomalies were observed anywhere on Kilauea on 23 February. However, an anomaly appeared in the vicinity of Pu'u 'O'o between 0643 and 0658 on 24 February, marking the return of active lava to the surface at Pu'u 'O'o.

Conclusions and Applications

Our analysis of episode 54 shows that the detection of thermal anomalies due to small areas (~0.2 km^2) of active lava in GOES data is possible. This means that given cloud-free conditions, effusive eruptions can be monitored every 15 minutes using GOES data. In addition, these data are freely available in near-real time, so that similar studies to the one presented here could be conducted on other volcanoes that are visible to GOES-8 and -9. Because these data can be processed in a few minutes, our analysis also shows that GOES data may be useful for hazard mitigation work as well as augmenting the chronology of an eruption. We plan to incorporate this new tool in our monitoring of Hawaiian volcanoes and hope that it will also prove to be useful in monitoring other volcanoes. To this end we automatically produce hot spot movies, an application to which the frequently collected GOES data is ideally suited. For Hawaii our movie covers a 3-day (~290 images) moving window which is updated with the latest image as soon as it is available [see http:// www.pgd.hawaii.edu /current /goes/]. We find that the movie is an effective way of analyzing the establishment and development of hot spots. Our software also extracts the Hawaii subscene from the full GOES scene, calibrates each band, carries out the necessary band subtraction, and converts the data to a generally readable format which can be used at the USGS Hawaiian Volcano Observatory.

Acknowledgments. We gratefully acknowledge the efforts of Joe Turk and Jeff Hawkins (Marine Meteorology Division, Naval Research Laboratory, Monterey, CA) in providing the GOES-9 digital data used in this effort, and of Harold Garbeil and Eric Pilger (HIGP/SOEST) for writing the automated processing software. This work was supported by NASA Grant NAG5-4395, awarded to the EOS Volcanology Team. This is HIGP contribution number 962 and SOEST contribution number 4541.

References

Glaze, L. S., P. W. Francis, S. Self, and D. A. Rothery, The 16 September 1986 eruption of Lascar volcano, north Chile: satellite investigations, *Bull. Volcanol.*, *51*, 149-160, 1989.

Harris, A. J. L., R. A. Vaughan, and D. A. Rothery, Volcano detection and monitoring using AVHRR data: the Krafla eruption, 1984, *Int. J. Remote Sensing*, *16*, 1001-1020, 1995a.

Harris, A. J. L., S. E. J. Swabey, and J. Higgins, Automated thresholding of active lavas using AVHRR data, *Int. J. Remote Sensing*, *16*, 3681-3686, 1995b.

Holasek, R. E., and S. Self, GOES weather satellite observations and measurements of the May 18, 1980, Mount St. Helens eruption, *J. Geophys. Res.*, *100*, 8469-8487, 1995.

Mouginis-Mark, P. J., H. Garbeil, and P. Flament, Effects of viewing geometry on AVHRR observations of volcanic thermal anomalies, *Remote. Sens. Environ.*, *48*, 51-60, 1994.

Rose, W. I., and D. J. Schneider, Satellite images offer aircraft protection from volcanic ash clouds, *Eos, Trans. AGU*, 77, 529-532, 1996.

Thornber, C. R., D. Sherrod, C. Heliker, J. Kauahikaua, F. Trusdell, M. Lisowski, and P. Okubo, Kilauea's ongoing eruption: Napau crater revisited after 14 years, *Eos, Trans. AGU*, 78, 329, 1997.

Wiesnet, D. R., and J. D'Aguanno, Thermal imagery of Mount Erebus from the NOAA-6 satellite, *Antarctic J. U.S.*, *17*, 32-34, 1982.

A. J. L. Harris, L. Keszthelyi, L. P. Flynn, and P. J. Mouginis-Mark, Hawaii Institute of Geophysics and Planetology, University of Hawaii, 2525 Correa Road, Honolulu, HI 96822. (e-mail: harris@kahana.pgd.hawaii.edu)

C. Thornber, J. Kauahikaua, D. Sherrod, and F. Trusdell, U.S. Geological Survey, Hawaiian Volcano Observatory, Hawaii National Park, Hawaii, HI 96718.

M. W. Sawyer and P. Flament, Department of Oceanography, University of Hawaii, 1000 Pope Road, Honolulu, HI 96822.

(Received September 5, 1997; accepted October 16, 1997.)